Molecular Pharmacology Fast Forward. Published on July 3, 2008 as doi:10.1124/mol.108.049395

MOL #49395

Keratinocyte-derived VEGF biosynthesis represents a pleiotropic side effect of PPARγ agonist troglitazone but not rosiglitazone and involves activation of p38 MAPK: implications for diabetes-impaired skin repair

Dana Schiefelbein, Oliver Seitz, Itamar Goren, Jan Philipp Dißmann,

Helmut Schmidt, Malte Bachmann, Robert Sader, Gerd Geisslinger,

Josef Pfeilschifter, and Stefan Frank

pharmazentrum frankfurt/ZAFES (D.S.; O.S.; I.G.; J.P.D.; H.S., M.B.; G.G., J.P.; S.F.)

Zentrum der Chirurgie (R.S.)

Klinikum der Johann Wolfgang Goethe-Universität, Theodor-Stern-Kai 7,

D-60590 Frankfurt am Main, Germany

Molecular Pharmacology Fast Forward. Published on July 3, 2008 as DOI: 10.1124/mol.108.049395
This article has not been copyedited and formatted. The final version may differ from this version.

Running title: thiazolidinediones and keratinocyte VEGF expression

Correspondence to:

Dr. Stefan Frank
pharmazentrum frankfurt/ZAFES
Institut für Allgemeine Pharmakologie und Toxikologie
Klinikum der JW Goethe-Universität Frankfurt/M.
Theodor-Stern-Kai 7
D-60590 Frankfurt/M., Germany
Tel.: 069-6301-6955
Fax: 069-6301-7942
E-MAIL: S.Frank@em.uni-frankfurt.de

number of text pages: 32

number of tables: 0

number of figures: 13

number of references: 44

number of words in *Abstract*: 222

number of words in *Introduction*: 485

number of words in *Discussion*: 1272

nonstandard abbreviations: *PPAR*, peroxisome proliferator-activated receptor; *VEGF*, vascular endothelial growth factor; *TZD*, thiazolidinedione

Molecular Pharmacology Fast Forward. Published on July 3, 2008 as DOI: 10.1124/mol.108.049395
This article has not been copyedited and formatted. The final version may differ from this version.

Abstract

The peroxisome proliferator-activated receptors (PPAR) represent pharmacological target molecules to improve insulin resistance in type 2 diabetes mellitus. Here we assessed a functional connection between pharmacological activation of PPAR and vascular endothelial growth factor (VEGF) expression in keratinocytes and during diabetes-impaired acute skin repair in *obese/obese* (*ob/ob*) mice. PPARβ/δ agonist L165,041 and PPARγ agonists ciglitazone and troglitazone, but not rosiglitazone, potently induced VEGF mRNA and protein expression from cultured keratinocytes. Inhibitor studies revealed a strong functional dependence of troglitazone- and L165,041-induced VEGF expression on p38 and p42/44 MAPK activation in keratinocytes. Rosiglitazone also induced activation of p38 MAPK, but failed to mediate activation of p42/44 MAPK in the cells. Functional ablation of PPARβ/δ and PPARγ from keratinocytes by small interfering RNA (siRNA) did not abrogate L165,041- and troglitazone-induced VEGF biosynthesis and suggested VEGF induction as a pleiotropic, PPAR-independent effect of both drugs in the cells. In accordance to the *in vitro* situation, we found activated p38 MAPK in wound keratinocytes from acute wounds of rosiglitazone- and troglitazone-treated diabetic *obese/obese* mice, whereas keratinocyte-specific VEGF protein signals were only prominent upon troglitazone treatment. In summary, our data from cell culture and wound healing experiments suggested p38 MAPK activation as a side effect of thiazolidinediones, however only troglitazone, but not rosiglitazone, appeared to translate p38 MAPK activation into a PPARγ-independent induction of VEGF from keratinocytes.

Molecular Pharmacology Fast Forward. Published on July 3, 2008 as DOI: 10.1124/mol.108.049395
This article has not been copyedited and formatted. The final version may differ from this version.

Introduction

Recent decades have shown a dramatic increase in obesity worldwide. Sedentary life style and consumption of high-caloric food represent the major causes for the obesity-'epidemic' in developed countries (Friedman, 2003). This obesity is associated with an increased risk to develop an insulin resistance and a type 2 diabetes mellitus. In addition to this concept, there is now strong evidence that immune responses and obesity are tightly connected and that insulin resistance has to be regarded as a functional consequence of adipose tissue-driven inflammatory processes (Hotamisligil, 2006).

Thiazolidinediones (TZD) represent a class of anti-diabetic drugs which are capable to improve insulin resistance in target tissues such as muscle and liver (Henry, 1997). In 1995, it has become clear that TZDs act through activation of the nuclear hormone receptor peroxisome proliferator-activated receptor (PPAR)γ (Lehmann et al., 1995). The PPAR family of transcription factors consists of two additional members: PPARα and PPARβ/δ, and all members heterodimerize with 9-*cis*-retinoic acid retinoid X receptors (RXR) (Kliewer et al., 1992; 1994). Insulin resistance now appears to be a consequence of the release of cyto- and adipokines from growing adipose tissue under conditions of obesity (Hotamisligil, 2006; Tilg and Moschen, 2006). TZDs interfere with the endocrine signaling process of adipocytes to muscle and liver and enhance insulin action in these organs through down-regulation of tumor necrosis factor (TNF)α and IL-6, and induction of the insulin-sensitizing hormone adiponectin in adipose tissue (Rangwala and Lazar, 2004). Interestingly, hyperlipidemia, representing an additional obesity-associated risk factor, can be improved by fibrates which activate PPARα (Staels and Fruchart, 2005).

Diabetes-associated severe ulcerations of the skin represent a serious problem of growing clinical importance. Diabetic ulcers still have a poor prognosis with high reulceration rates and a high mortality after limb amputations (Faglia et al., 2001). Besides their metabolic

Molecular Pharmacology Fast Forward. Published on July 3, 2008 as DOI: 10.1124/mol.108.049395
This article has not been copyedited and formatted. The final version may differ from this version.

functions, interestingly, PPARα, β/δ and γ have been shown to be also involved in the homeostatic regulation of normal and injured skin [for a review see Michalik and Wahli, 2007). Epidermal keratinocytes express all three PPAR isoforms (Rivier et al., 1998). In these cells, PPARβ/δ is the major isoform, whereas PPARα and PPARγ are increased and functionally connected to keratinocyte differentiation in humans and mice (Rivier et al., 1998; Komuves et al., 2000; Mao-Qiang et al., 2004). By contrast to PPARγ, which remains hardly detectable upon skin wounding, PPARα and β/δ are reactivated in wound margin keratinocytes during acute healing in mice (Michalik et al., 2001). Keratinocytes represent a major source of VEGF in skin wounds (Brown et al., 1992) and VEGF expression is induced by cytokines and growth factors in the cells (Frank et al., 1995). In this study, we investigated the potency of PPAR agonists to interfere with keratinocyte-derived VEGF expression. PPARγ agonist troglitazone, but not rosiglitazone, potently induced keratinocyte VEGF expression, however, our data constitute evidence that troglitazone-mediated induction of VEGF expression was independent from PPARγ but functionally connected to p38 MAPK activation in cultured keratinocytes.

Materials and methods

Animals. Female C57BL/6J-*ob/ob* mice were obtained from Charles River WIGA (Sulzfeld, Germany) and maintained under a 12h light/12h dark cycle at 22°C until they were 10 weeks of age. At this time they were caged individually, monitored for body weight and wounded as described below.

Treatment of mice. Mice were treated with rosiglitazone (Avandia®, 5 mg/kg/day) or troglitazone (5 mg/kg/day) twice a day (6 a.m., 6 p.m.) by gastrogavage for the indicated time points. The drug was freshly homogenized in 0,5 % methylcellulose (Fluka, Sigma-Aldrich,

Molecular Pharmacology Fast Forward. Published on July 3, 2008 as DOI: 10.1124/mol.108.049395
This article has not been copyedited and formatted. The final version may differ from this version.

Seelze, Germany) prior to oral administration. Treatment of mice with 0.5 % methylcelluose alone served as a control. Rosiglitazone (Avandia®) was from GlaxoSmithKline Consumer Healthcare, Bühl, Germany), troglitazone was from Axxora (Lörrach, Germany).

Wounding of mice. Wounding of mice was performed as described previously (Stallmeyer et al., 1999; Frank et al., 1999). Briefly, mice were anesthetized with a single i.p. injection of ketamine (80 mg/kg body weight)/xylazine (10 mg/kg body weight). Six full-thickness wounds (5 mm in diameter, 3-4 mm apart) were made on the back of each mouse by excising the skin and the underlying *panniculus carnosus*. An area of 7-8 mm in diameter, which included the granulation tissue and the complete epithelial margins, was excised at the indicated time points for analysis. As a control, a similar amount of skin was taken from the backs of nonwounded mice. For each experimental time point, tissue from four wounds each from three animals (n=12 wounds, RNA analysis) and from two wounds each from three animals (n=6 wounds, protein analysis) were combined and used for RNA and protein preparation. All animal experiments were carried out according to the guidelines and were approved by the local Ethics Animal Review Board.

RNA isolation and RNase protection analysis. RNA isolation and RNase protection assays were carried out as described previously (Frank et al., 1999; Chomczynski and Sacchi, 1987). The cDNA probes were cloned using RT-PCR. The murine probes corresponded to nt 139-585 (for vascular endothelial growth factor [VEGF], S38083), nt 1499-1779 (for PPARβ/δ, NM_006238) and nt 163-317 (for GAPDH, NM002046). The human probes corresponded to nt 1362-1516 (for VEGF, NM_001025370.1) and nt 961-1070 (for GAPDH, M33197), respectively.

Immunohistochemistry. Mice were wounded as described above. Animals were sacrificed at day 5 after injury. Complete wounds were isolated from the back and fixed in formalin. Bisected wounds were embedded in paraffin. Immunohistochemistry from four µm

Molecular Pharmacology Fast Forward. Published on July 3, 2008 as DOI: 10.1124/mol.108.049395
This article has not been copyedited and formatted. The final version may differ from this version.

deparaffinized serial sections was performed as described (Stallmeyer et al., 1999). Sections were stained with the avidin-biotin-peroxidase complex system using 3,3-diaminobenzidine-tetrahydrochloride as a chromogenic substrate. Nuclei were counterstained with hematoxylin. The antibody directed against murine VEGF was from Santa Cruz, Heidelberg, Germany. The phospho-specific anti-p38 MAPK antibody was obtained from Cell Signalling, New England Biolabs (Frankfurt, Germany).

Cell culture. Human HaCaT epidermal keratinocytes (Boukamp et al., 1988) were grown to confluency in Dulbecco's modified Eagles's medium (DMEM) (Gibco-BRL, Eggenstein, Germany). Human primary keratinocytes were isolated according to a protocol from PromoCell (www.promocell-academy.com) and cultured in keratinocyte growth medium 2 (PromoCell, Heidelberg, Germany). The murine macrophage cell line RAW264.7 was cultured in RPMI medium (Gibco-BRL). Confluent keratinocytes were subsequently treated with epidermal growth factor (EGF, 10 ng/ml), ciglitazone (0,1 - 25 µM), troglitazone (0,1 - 25 µM), rosiglitazone (0,1 - 50 µM), L165,041 (0,1 - 50 µM), WY14643 (50 µM), clofibrate (500 µM) in the presence or absence of 200 nM wortmannin (WTM), 10 µM U0126, 5 µM SB203580, or 10 µM actinomycin D (Act D) for the indicated periods of time. RAW264.7 cells were stimulated with lipopolysaccharide (LPS, 200 ng/ml) and interferon-γ (IFN-γ, 2 ng/ml). EGF and IFN-γ were purchased from Roche Biochemicals (Mannheim, Germany). WTM and SB203580 were obtained from Calbiochem (Darmstadt, Germany) and U0126 was from Alexis (San Diego, U.S.A.). Ciglitazone, troglitazone, L165,041, WY14643 and clofibrate were obtained from Merck (Darmstadt, Germany). Rosiglitazone was from Axxora (Lörrach, Germany). LPS was from Sigma (Taufkirchen, Germany).

Nitrite determination in cell culture supernatants. Nitrite, a stable nitric oxide (NO) oxidation product, was determined in cell culture supernatants using the Griess reaction (Green et al., 1982). Briefly, cleared supernatants were mixed with 20 µl sulfanilamide

Molecular Pharmacology Fast Forward. Published on July 3, 2008 as DOI: 10.1124/mol.108.049395
This article has not been copyedited and formatted. The final version may differ from this version.

(dissolved in 1.2 M HCl) and 20 µl N-naphtylethylenediamine dihydrochloride. After 5 min, the absorbance was measured at 540 nm.

Determination of cell viability. Viability of cultured keratinocytes was assessed using the 3-(4,5-Dimethylthiazol-2-yl)-2,5-diphenyltetrazolium (MTT) assay following a published protocol (Mosmann et al., 1983).

Enzyme-linked immunosorbent assay (ELISA). Quantification of human $VEGF_{165}$ protein from keratinocyte cell culture supernatants was performed using the human VEGF ELISA kit (Biosource, Nivelles, Belgium).

Preparation of protein lysates and immunoblot analysis. Keratinocyte cell culture samples and murine skin were homogenized as described (Goren et al., 2006). Twenty to fifty micrograms of total protein lysate was separated using sodium dodecyl sulfate (SDS)-gel electrophoresis, and specific proteins were detected using antisera directed against total Akt, phospho-Akt (Ser473), phospho-p38 MAPK (Thr180, Tyr182), phospho-p42/44 MAPK (Thr202, Tyr204) (Cell Signalling, New England Biolabs, Frankfurt, Germany), PPARγ (Santa Cruz, Heidelberg, Germany) and β-actin (Sigma). A secondary antibody coupled to horseradish peroxidase and the ECL detection system was used to visualize the proteins of interest. Phenylmethylsulfonyl fluoride, aprotinin, NaF, Na_2VO_4 and dithiothreitol were from Sigma. Ocadaic acid and leupeptin were from BioTrend (Köln, Germany) and the ECL detection system was obtained from Amersham (Freiburg, Germany).

Silencing of PPARγ and PPARβ/δ expression by siRNA. 2×10^5 HaCaT keratinocytes were grown in 6-well plates to reach 40 - 60% confluency. Cells were subsequently transfected twice with the respective small interfering RNA (siRNA, 50 nM final concentration) using oligofectamine® (Invitrogen, Karlsruhe, Germany) and OptiMEM (Invitrogen) as described by the manufacturer.

Molecular Pharmacology Fast Forward. Published on July 3, 2008 as DOI: 10.1124/mol.108.049395
This article has not been copyedited and formatted. The final version may differ from this version.

Determination of rosiglitazone and troglitazone in mouse plasma samples by LC-MS/MS. Aliquots of mouse plasma samples were extracted by methanol/water (50:50 v/v) precipitation. Pioglitazone and ciglitazone were used as internal standards for rosiglitazone and troglitazone, respectively. HPLC analysis was done under gradient conditions using a Luna C18(2) column (Phenomenex, Aschaffenburg, Germany). MS and MS/MS analyses were performed on a 4000 Q TRAP triple quadrupole mass spectrometer with a Turbo V source (Applied Biosystems, Darmstadt, Germany) in the negative ion mode. Precursor-to-product ion transitions of m/z 356→42 for rosiglitazone, 440→42 for troglitazone, 355→42 for pioglitazone and m/z 332→42 for ciglitazone were used for the MRM with a dwell time of 150 ms. Concentrations of the calibration standards, quality controls and unknowns were evaluated by Analyst software (version 1.4; Applied Biosystems, Darmstadt, Germany). Variations in accuracy and intra-day and inter-day precision (n = 6 for each concentration, respectively) were < 15% over the range of calibration.

Statistical analysis. Data are shown as means ± standard deviation (SD). Data analysis was carried out using the unpaired Student's *t* test with raw data. Statistical comparison between more than two groups was carried out by analysis of variance (ANOVA, Dunnett's method).

Results

Troglitazone and L165,041, but not rosiglitazone potently induce VEGF expression in keratinocytes. Epidermal keratinocytes express all three PPAR subtypes (Rivier et al., 1998). As angiogenesis is central to skin repair (Singer and Clark, 1999; Eming and Krieg, 2006) and keratinocytes are well-known producers of VEGF at the wound site (Brown et al., 1992) and *in vitro* (Frank et al., 1995), we tested the potency of diverse PPAR agonists to drive VEGF expression in keratinocytes. The PPARγ agonists troglitazone (**Figure 1a**), ciglitazone

Molecular Pharmacology Fast Forward. Published on July 3, 2008 as DOI: 10.1124/mol.108.049395
This article has not been copyedited and formatted. The final version may differ from this version.

(Supplemental Figure S1) and the PPARβ/δ agonist L165,041 (**Figure 1c**) were potent inducers of VEGF mRNA (*upper and middle panel*) and protein (*lower panel*) expression in cultured human HaCaT keratinocytes. By contrast, the PPARγ agonist rosiglitazone failed to induce VEGF expression in the cells at low (0,1 - 25 μM, data not shown) and even at highest concentrations (**Figure 1b**). Interestingly, the dose-response experiment revealed that the PPARγ agonists troglitazone and ciglitazone or the β/δ agonist L165,041 mediated an 'on/off'-phenomenon with respect to VEGF expression at higher concentrations (glitazones: 25 μM; L165,041: 50 μM) (**Figure 1a,c;** Supplemental Figure S1). By contrast, PPARα agonists WY14634 (50 μM) and clofibrate (500 μM) did not induce VEGF mRNA and protein expression in keratinocytes even at highest concentrations (data not shown).

As a next step, we determined the kinetics of VEGF expression in keratinocytes using the effective concentration of respective PPARγ (troglitazone and ciglitazone only; as rosiglitazone did not induce VEGF) and β/δ agonists. PPARγ agonists troglitazone (**Figure 2a**) and ciglitazone (Supplemental Figure S2) or the PPARβ/δ agonist L165,041 (**Figure 2b**) mediated a steady increase in VEGF mRNA (*upper panels*) and protein (*lower panels*) expression in keratinocytes. In contrast to rosiglitazone (**Figure 1b**), the PPAR agonists troglitazone and L165,041 induced a dramatic stimulation of VEGF mRNA (20- to 60-fold) and the release of large amounts of VEGF protein (5 to 20 ng/ml) into the cell culture supernatants.

To test the bioactivity of rosiglitazone, we assessed the ability of this drug to suppress the pro-inflammatory stimulation of murine macrophages *in vitro*. LPS and IFN-γ, which classically trigger macrophage inflammatory activity (Gordon, 2003), potently mediated the accumulation of nitrite in cell culture supernatants of stimulated RAW264.7 macrophages. Nitrite represents a reliable readout for inducible nitric oxide synthase activity. Rosiglitazone

Molecular Pharmacology Fast Forward. Published on July 3, 2008 as DOI: 10.1124/mol.108.049395
This article has not been copyedited and formatted. The final version may differ from this version.

(50 µM) turned out to be effective, as the drug significantly reduced the production of nitrite from activated RAW264.7 macrophages (**Figure 3**).

In addition, **Figure 4** demonstrates that also human primary keratinocytes responded to troglitazone and L165,041 treatment by increased VEGF mRNA (**a**) and protein (**b**) expression. EGF, which is described as a potent inducer of VEGF expression from human keratinocytes (Frank et al., 1995) has been used as positive control in our experimental setting.

Troglitazone and L165,041 induce VEGF gene transcription. To investigate whether the increase in VEGF mRNA was due to an interference of the respective drug with transcriptional or post-transcriptional control mechanisms, we stimulated actinomycin D (Act D, 10 µM) pretreated keratinocytes with troglitazone or L165,041. In this experimental setting, we did not observe any increase in VEGF mRNA upon stimulation (data not shown). However, troglitazone or L165,041 might contribute to VEGF production by stabilizing the transcriptionally induced VEGF mRNA species. To test this hypothesis, we stimulated the cells with the respective drug for 16 h to induce VEGF mRNA and subsequently added Act D to shut off active transcription. EGF stimulation was performed as control (Frank et al., 1995). As shown in **Figure 5 (***upper panel***)**, we observed a rapid decrease of induced VEGF mRNA following Act D-mediated inhibition of transcriptional activity. Independent from the individual potency of the respective drug to induce VEGF expression, we observed a comparable half-life of VEGF mRNA of about 4 h for troglitazone, L165,041 or EGF, respectively. **Figure 5** (*lower panel*) shows the respective time controls (16 h and 24 h) for drugs and EGF, which clearly show that VEGF mRNA was not reduced in the absence of Act D.

Troglitazone- and L165,041-induced VEGF expression is independent from PPAR activation. As given in **Figure 6**, inhibitor experiments strongly argue for MAPK activation

Molecular Pharmacology Fast Forward. Published on July 3, 2008 as DOI: 10.1124/mol.108.049395
This article has not been copyedited and formatted. The final version may differ from this version.

as the functional basis of troglitazone-mediated VEGF expression in keratinocytes. Notably, inhibition of either p42/44 (by U0126) or p38 (by SB203580) MAPK nearly completely abrogated troglitazone-induced expression of VEGF mRNA in keratinocytes, whereas inhibition of PI3K by wortmannin had no effect (**Figure 6a,** *upper panels*). As a consequence, we observed a marked reduction of troglitazone-induced VEGF protein upon inhibition of p42/44 and p38 MAPK at the early 16 h experimental time point, and inhibition of VEGF protein expression remained significantly reduced even after 24 h of stimulation (**Figure 6a,** *lower panel*). In addition, induction effects of the PPARβ/δ agonist L165,041 on keratinocyte VEGF mRNA (**Figure 6b,** *upper panels*) and protein (**Figure 6b,** *lower panel*) expression appeared to be sensitive to inhibition of PI3K or p42/44 and p38 MAPK activation.

In accordance to wortmannin insensitive VEGF induction by troglitazone, we did not observe an increased phosphorylation of protein kinase B(PKB)/Akt which represents a target of active PI3K (Franke et al., 1995) (data not shown). In contrast, troglitazone mediated a strong phosphorylation and thus activation of both p38 and p42/44 MAPK (**Figure 7a**). The PPARγ agonist rosiglitazone did not induce VEGF expression in keratinocytes (**Figure 1b**), however, the drug shared its capability to potently induce p38 MAPK activation with troglitazone. Rosiglitazone failed to mediate p42/44 MAPK activation (**Figure 7a**). Activation of the MAPKs by the assessed drugs in keratinocytes appeared to be independent from a cellular response towards stress or toxicity, as a cell viability assay showed only moderate changes in cell survival upon drug exposure (**Figure 7b**).

To unequivocally prove a PPAR-independent mode of action for troglitazone- and L165,041-induced VEGF expression in keratinocytes, we used a siRNA approach to specifically knock-down PPAR expression in the cells. As shown in **Figure 8a**, PPARγ-specific siRNA was able to abrogate the observed constitutive expression of PPARγ protein. For unknown reasons, we consistently observed an increase of PPARγ expression in keratinocytes transfected with the

Molecular Pharmacology Fast Forward. Published on July 3, 2008 as DOI: 10.1124/mol.108.049395
This article has not been copyedited and formatted. The final version may differ from this version.

scrambled control RNA. Troglitazone mediated a robust induction of keratinocyte VEGF expression in the absence of functional PPARγ (**Figure 8a**), clearly demonstrating that specific binding of troglitazone to PPARγ must not be involved in its capability of stimulating VEGF expression in keratinocytes. In accordance, the siRNA-specific knock-down of PPARβ/δ in the cells did not interfere with L165,041-induced VEGF expression, again suggesting a receptor-independent mechanism also for L165,041 (**Figure 8b**). Please note that we were forced to control the PPARβ/δ knock-down at the mRNA level, as we failed to convincingly show a PPARβ/δ protein expression with different commercially available antibodies (data not shown).

Opposite effects of PPARγ agonists rosiglitazone and troglitazone on wound keratinocytes in diabetes-impaired skin wounds. PPARγ is only hardly detectable in acute wound tissue and appears to be of minor importance for tissue repair (Michalik et al., 2001). However, as we had demonstrated the robust VEGF induction to be independent from PPARγ in keratinocytes (**Figures 6, 8**), it was interesting to assess a potential therapeutic action of PPARγ agonists to improve the strongly impaired angiogenic process in diabetic wound tissue (Frank et al., 1995; Eming and Krieg, 2006; Stallmeyer et al., 2001; Kämpfer et al., 2001) by stimulating VEGF release from wound keratinocytes. **Figure 9** demonstrates the marked loss of VEGF protein expression in acute wound tissue of diabetic *ob/ob* mice. To improve these disturbed conditions, we treated wounded diabetic *ob/ob* mice orally with the PPARγ agonists rosiglitazone or troglitazone, respectively. Liquid chromatography/mass spectrometry/mass spectrometry (LC/MS/MS) analysis of blood serum from treated animals revealed the high bioavailability of both drugs: oral administration of 5 mg/kg/day rosiglitazone resulted in average blood serum levels of 12,5 µg ± 2,5 µg rosiglitazone/ml; oral administration of 5 mg/kg/day troglitazone led to average blood serum levels of 0,9 µg ± 0,3 µg troglitazone/ml.

Molecular Pharmacology Fast Forward. Published on July 3, 2008 as DOI: 10.1124/mol.108.049395
This article has not been copyedited and formatted. The final version may differ from this version.

Upon treatment of animals, we determined expression levels of VEGF mRNA from complete acute wound tissue isolated from mock- and rosiglitazone-treated *ob/ob* mice. Only wound tissue from mock-treated animals was characterized by significantly increased VEGF mRNA levels compared to non-wounded skin (**Figure 10a**). Although significant in the ANOVA statistical analysis, the difference between mock- and rosiglitazone-administered mice appeared only very moderate in early wounds (**Figure 10a**, *1d wound tissue*). However, the differences in VEGF mRNA levels upon rosiglitazone treatment turned out to become more pronounced during ongoing repair (**Figure 10a**, *5d wound tissue*). As a next step, we separated total wound tissue into the wound margin (*wm*, enriched for wound margin keratinocytes as potential producers of VEGF) and inner wound (*iw*, contains the granulation tissue) compartments prior to RNA isolation. Strengthening our data from total wound tissue, we found a marked reduction of VEGF mRNA levels restrictively only at the wound margins (*wm*) in rosiglitazone-treated *ob/ob* mice (**Figure 10b**). Immunohistochemistry data on wound tissue from *ob/ob* mice revealed a detailed insight into the interference of rosiglitazone with tissue repair. In line with mRNA data from wound margin (*wm*) tissue (**Figure 10b**), we observed marked signals of immunoreactive VEGF protein in wound margin keratinocytes of mock-treated *ob/ob* mice (**Figure 10c** and **Figure 12**, *upper panel*). Rosiglitazone appeared to interfere with VEGF synthesis in impaired wound tissue in two ways: First by reducing the expression of total VEGF protein in wound keratinocytes (VEGF-specific signals were reduced) and second by inhibiting overall keratinocyte proliferation, as wound margin epithelia of rosiglitazone-administered mice exhibited an atrophied morphology (**Figure 10c** and **Figure 12**, *upper panel*). This was in contrast to the effects mediated by troglitazone treatment of mice. Reflecting the *in vitro* potency to induce VEGF expression in keratinocytes (**Figure 1,2**), troglitazone mediated a robust VEGF expression in wound margin epithelia (**Figure 12**, *upper panel*). Here, it is noteworthy that VEGF-specific signals in wound keratinocytes from troglitazone-treated *ob/ob* mice appeared even elevated compared to

Molecular Pharmacology Fast Forward. Published on July 3, 2008 as DOI: 10.1124/mol.108.049395
This article has not been copyedited and formatted. The final version may differ from this version.

mock-treated animals. Moreover, sizes of wound margin epithelia were also not reduced by troglitazone treatment (**Figure 12**, *upper panel*).

Immunoblots using wound lysates revealed obvious differences in the activation of MAPKs at the wound site upon different drug regimen. Whereas levels of activated p38 were reduced in the presence of unaltered p42/44 phosphorylation in wounds of rosiglitazone- *versus* mock-treated mice, we found an induction of p42/44 activation and no difference in p38 activation in wound tissue of troglitazone-treated animals (**Figure 11**). However, these immunoblots from wound lysates reflected all cell types at the wound site: This is a major disadvantage with respect to our experiments, which aimed to functionally connect actions of PPARγ agonists specifically to keratinocytes. To circumvent this problem, we performed immunohistochemistry of wound tissue to allow an analysis of p38 activation in wound keratinocytes. As shown in **Figure 12**, wound margin keratinocytes of troglitazone-treated mice expressed a robust presence of activated p38. The presence of phosphorylated p38 appeared even enhanced compared to mock-treated animals, as nearly all keratinocytes exhibited a nuclear presence of phosphorylated p38 upon troglitazone treatment. The observed reduction of wound margin epithelia upon rosiglitazone treatment (**Figure 10,12**) was also paralleled by an activation of p38, as again nearly all keratinocytes of the reduced epithelia stained for the phosphorylated kinase. It is important to note here, that our histology-based data were in accordance to our *in vitro* findings from cultured keratinocytes: both PPARγ agonists had been inducers of p38 activation, but only troglitazone was capable to mediate a PPARγ-independent induction of VEGF expression in the cells.

Here, we further analyzed wound granulation tissue and scab for activated p38. We did so to explain the different signals for activated p38 in immunoblots and histologies: rosiglitazone-treated *ob/ob* mice showed an overall reduction, troglitazone-treated mice any change in p38 activation in wound lysates (**Figure 11**) in the presence of a significant phospho-p38 staining

Molecular Pharmacology Fast Forward. Published on July 3, 2008 as DOI: 10.1124/mol.108.049395
This article has not been copyedited and formatted. The final version may differ from this version.

in keratinocytes (**Figure 12,** *second panel*). Lower levels of activated p38 in immunoblots of total wound tissue upon rosiglitazone treatment appeared to reflect an overall reduction of phosphorylated p38 in wound macrophages (**Figure 12**, *third panel*). According to the immunoblot (Figure 11), troglitazone did not reduce activated p38 in wound macrophages compared to mock-treated mice (**Figure 12**, *third panel*). Polymorphonuclear neutrophils did not contribute to this regulation, as this cell type did not express activated p38 (**Figure 12**, *lower panel*). In summary, the action of both PPARγ agonists on wound macrophages might explain, at least partially, the observed status of p38 activation in total wound tissues of TZD-treated mice.

PPARγ agonists do not interfere with cytokine- and growth factor-induced VEGF expression in keratinocytes. Finally, we tested the potency of rosiglitazone and troglitazone to interfere with keratinocyte responses towards wound-derived mediators such as cytokines and EGF. This was important, as VEGF expression from wound keratinocytes in rosiglitazone (reduced VEGF expression) and troglitazone (robust VEGF expression)-treated *ob/ob* mice might not only be a result of the observed PPARγ-independent effects, but might also be based on a functional interaction with responses of wound keratinocytes towards wound-derived mediators. To this end, we stimulated keratinocytes with submaximal concentrations of cytokines and EGF to enable a modulation of induced VEGF expression by the drugs. We determined the EC_{50} for cytokine (combination of TNFα: 0,25 ng/ml, IL-1β: 0,5 ng/ml; IFNγ: 0,1 ng/ml) and EGF (2 ng/ml) stimulation (**Figure 13**, *upper panels*). Subsequently, we stimulated keratinocytes with the assessed EC_{50} of cytokines and EGF in the presence of increasing amounts of rosiglitazone and troglitazone, respectively. We did not observe any changes in cytokine- and EGF-induced VEGF expression in the presence of the respective PPARγ agonist (**Figure 13**, *lower panels*).

Molecular Pharmacology Fast Forward. Published on July 3, 2008 as DOI: 10.1124/mol.108.049395
This article has not been copyedited and formatted. The final version may differ from this version.

Discussion

The family of peroxisome proliferator-activated receptors (PPAR) appears to be an attractive group of proteins with promising novel therapeutical applications. Especially, PPARγ-activating TZDs have been developed to improve type 2 diabetes mellitus-associated insulin resistance (Staels and Fruchart, 2005). Interestingly, PPARγ might serve an integrative function at the interface between metabolic regulation and tissue movements. This notion appears to be even more important, as it has become evident that metabolism and inflammation are functionally connected through mechanisms of innate immunity (Hotamisligil, 2006). PPARγ participates in the control of fatty acid metabolism and the release of cytokines and adipokines from white adipose tissue (Rangwala and Lazar, 2004). In animal models of obesity, circulating levels of fatty acids (Delarue and Magnan, 2007), cytokines (Hotamisligil, 2006) and adipokines (Tilg and Moschen, 2006) are functionally connected to obesity-induced insulin resistance. At least in mice, skin tissue is known to differentially express all isoforms of PPAR (Michalik and Wahli, 2007) as well as representing an organ system susceptible of developing an obesity-mediated insulin resistance (Goren et al., 2006).

Diabetic conditions severely impair the healing process of cutaneous wounds in human individuals (Falanga, 2005) and in mice (Goren et al., 2003, 2006; Frank et al., 2000). In this context, it was tempting to argue for a possible function of therapeutically mediated PPAR activation to improve tissue movements during skin repair. In this study, we focussed on the expression of VEGF for following reasons: the expression of VEGF is markedly reduced in diabetes-impaired wounds (Frank et al., 1995), keratinocytes represent the principal source of VEGF during skin repair (Brown et al., 1992), and express PPARα, β/δ and γ isoforms (Michalik and Wahli, 2007).

Molecular Pharmacology Fast Forward. Published on July 3, 2008 as DOI: 10.1124/mol.108.049395
This article has not been copyedited and formatted. The final version may differ from this version.

Actually, both PPARα agonists clofibrate and WY14643 completely failed to induce VEGF in HaCaT keratinocytes. Our observation is supported by findings from an epithelial colon carcinoma cell line, where clofibrate and WY14643 were even potent suppressors of phorbolester-induced VEGF and Cox-2 expression. Interestingly, both substances inhibited DNA binding of activator protein-1 (AP-1) and thus transcriptional activation of VEGF and Cox-2 in a PPARα-dependent manner (Grau et al., 2006). By contrast, both the PPARβ/δ agonist L165,041 and the PPARγ agonists troglitazone and ciglitazone mediated a robust induction of VEGF mRNA and protein expression from cultured keratinocytes. This observation is in good accordance to recent findings in diverse cellular systems. Myofibroblasts exhibit a PPARγ-dependent biosynthesis of VEGF upon treatment with troglitazone and 15-deoxy-prostaglandin J2. In these cells, PPARγ-induced VEGF increase was functionally coupled to a decrease of NFκB activity (Chintalgattu et al., 2007). Additionally, bovine articular chondrocytes have been shown to up-regulate VEGF via oxidized low-density lipoprotein (ox-LDL)-mediated PPARγ activation (Kanata et al., 2006). However, the specific PPARγ inhibitor GW9662 suppressed ox-LDL-induced VEGF expression in chondrocytes, providing evidence that PPARγ activation was, in contrast to keratinocytes, pivotal to VEGF expression. Nevertheless, the PPARγ agonist rosiglitazone failed to induce VEGF expression in keratinocytes, suggesting a different profile of pleiotropic actions for this member of the TZD family of drugs. Interestingly, it has been reported for several years that especially rosiglitazone provides anti-angiogenic effects in endothelial and epithelial cells. In accordance to the failure of rosiglitazone to stimulate VEGF expression in keratinocytes (this study), it is noteworthy that this drug exerted anti-angiogenic properties in particular by a marked reduction of VEGF biosynthesis during physiological processes such as endometrium-driven uterine angiogenesis (Peeters et al.,

Molecular Pharmacology Fast Forward. Published on July 3, 2008 as DOI: 10.1124/mol.108.049395
This article has not been copyedited and formatted. The final version may differ from this version.

2005) as well as during pathophysiological processes such as angiogenesis in tumor growth and metastasis (Panigrahy et al., 2002).

There is growing evidence that activation of PPARβ/δ stimulates VEGF release in close functional connection to inhibition of apoptosis and stimulation of proliferation in human endothelial cells (Piqueras et al., 2007), colon carcinoma cells (Wang et al., 2006), and also keratinocytes (Di-Poi et al., 2002). The potential of PPARβ/δ to trigger VEGF release in close functional connection to cell survival in a colon cancer cell line must be critically evaluated in the context of cancer development. By contrast, the ability of activated PPARβ/δ to drive VEGF expression (this study) and cell survival in keratinocytes by activation of PKB/Akt1 (Di-Poi et al., 2002) might be of functional importance in skin repair, where keratinocytes drive angiogenic processes via VEGF release (Brown et al., 1992; Frank et al., 1995) and cover the wound site from proliferative epithelia located at the margins of the wound (Singer and Clark, 1999).

In addition, it was reasonable and interesting to assess whether the observed unequal VEGF-stimulating capabilities of individual TZDs in cultured keratinocytes, even despite the observed independence of this process from binding to PPARγ, might also be transferred into diabetes-impaired wound conditions associated with disturbed angiogenic processes (Frank et al., 1995; Eming and Krieg, 2006; Kämpfer et al., 2001). Unfortunately, a functional role for PPARγ in skin repair remains still unresolved, especially as this receptor isoform was only hardly detectable in skin tissue upon injury (Michalik et al., 2001). Moreover, also the role of PPARγ in the control of keratinocyte proliferation and differentiation still remains complex (Michalik and Wahli, 2007). The TZD ciglitazone mediated differentiation in human keratinocytes *in vitro*, as assessed by the induction of the typical keratinocyte differentiation markers involucrin and transglutaminase 1. A PPARγ-mediated process of differentiation could also be induced in murine epidermis, as ciglitazone induced the expression of

Molecular Pharmacology Fast Forward. Published on July 3, 2008 as DOI: 10.1124/mol.108.049395
This article has not been copyedited and formatted. The final version may differ from this version.

keratinocyte differentiation markers loricrin and filaggrin in wildtype but not in PPARγ null keratinocytes in mice (Mao-Qiang et al., 2004). In addition, also PPARγ-independent effects appear to contribute to the TZD-mediated cellular decisions towards differentiation, as troglitazone caused a PPARγ-independent inhibition of keratinocyte proliferation by abrogation of cyclin D1 expression (He et al., 2004). In accordance to other reported PPARγ-independent mechanisms of TZDs in keratinocytes, we found that inhibition of p38 and p42/44 MAPK and not a functional ablation of PPARγ by siRNA abrogated TZD-stimulated VEGF expression in the cells. This observation confirms the findings of a most recent report on keratinocytes showing that troglitazone-induced Cox-2 expression did not involve PPARγ but p42/44 activation (He et al., 2006).

Interestingly, our experiments on TZD actions in acute wound healing in diabetic *ob/ob* mice basically support our major findings obtained from cultured keratinocytes: troglitazone and rosiglitazone both activated p38 MAPK in the cells, whereas the failure to induce VEGF expression was restricted to rosiglitazone only. This observation was quite interesting, as it again demonstrated potent differences in pleiotropic actions associated with drugs belonging to the same class of substances. In particular, those differences between troglitazone, which was withdrawn from the market in 2000 due to its drug-induced side effects, and rosiglitazone, which is still considered safe and of current therapeutic use, might contribute to the overall safety of individual members of the TZD family of drugs. In addition, our data from diabetes-impaired wound tissue *in vivo* suggested a rosiglitazone-mediated inhibition of wound keratinocyte proliferation, probably via activation of PPARγ (Mao-Qiang et al., 2004). Thus, it is reasonable to argue that the reduced VEGF expression from wound margin epithelia upon rosiglitazone treatment might be partially explained by decreased keratinocyte cell numbers. By contrast, troglitazone did not interfere with the size of wound margin epithelia, revealing an additional difference between both TZD drugs. Remarkably, the

Molecular Pharmacology Fast Forward. Published on July 3, 2008 as DOI: 10.1124/mol.108.049395
This article has not been copyedited and formatted. The final version may differ from this version.

functional connection between troglitazone and VEGF expression via activation of p38 and p42/44 MAPK in cultured keratinocytes appeared to be a key regulatory mechanism in VEGF biosynthesis also in wound keratinocytes *in vivo*, as we could observe an ubiquitous appearance of activated p38 MAPK in VEGF-expressing wound margin keratinocytes. In summary, our data from cell culture and wound healing experiments suggested p38 MAPK activation as a side effect of TZDs, however only troglitazone, but not rosiglitazone, appeared to translate p38 MAPK activation into a PPARγ-independent induction of VEGF from keratinocytes.

References

Boukamp P, Petrissevska RT, Breitkreuz D, Hornung J, Markham A and Fusenig NE (1988) Normal keratinization in a spontaneously immortalized aneuploid human keratinocyte cell line. *J Cell Biol* 106:761-771.

Brown LF, Yeu KT, Berse B, Yeo TK, Senger DR, Dvorak HF and Van de Water L (1992) Expression of vascular permeability factor (vascular endothelial growth factor) by epidermal keratinocytes during wound healing. *J Exp Med* 176:1375-1379.

Chintalgattu V, Harris GS, Akula SM and Katwa LC (2007) PPAR-gamma agonists induce the expression of VEGF and its receptors in cultured cardiac myofibroblasts. *Cardiovasc Res* 74:140-150.

Chomczynski P and Sacchi N (1987) Single-step method of RNA isolation by acid guanidinium thiocyanate-phenol-chloroform extraction. *Anal Biochem* 162:156-159.

Delarue J and Magnan C (2007) Free fatty acids and insulin resistance. *Curr Opin Clin Nutr Metab Care* 10:142-148.

Di-Poi N, Tan NS, Michalik W, Wahli W and Desvergne B (2002) Antiapoptotic role of PPARbeta in keratinocytes via transcriptional control of the Akt1 signaling pathway. *Mol Cell* 10:721-733.

Eming SA and Krieg T (2006) Molecular mechanisms of VEGF-A action during tissue repair. *J Invest Dermatol Symp Proc* 11:79-86.

Faglia E, Favales F and Morabito A (2001) New ulceration, new major amputation, and survival rates in diabetic subjects hospitalized for foot ulceration from 1990 to 1993: a 6.5 year follow-up. *Diabetes Care* 24:78-83.

Falanga V (2005) Wound healing and its impairment in the diabetic foot. *Lancet* 366:1736-1743.

Frank S, Hübner G, Breier G, Longaker MT, Greenhalgh DG and Werner S (1995) Regulation of vascular endothelial growth factor expression in cultured keratinocytes. Implications for normal and impaired wound healing. *J Biol Chem* 270:12607-12613.

Frank S, Stallmeyer B, Kämpfer H, Kolb N and Pfeilschifter J (1999) Nitric oxide triggers enhanced induction of vascular endothelial growth factor expression in cultured keratinocytes (HaCaT) and during cutaneous wound repair. *FASEB J* 13:2002-2014.

Frank S, Stallmeyer B, Kämpfer H, Kolb N and Pfeilschifter J (2000) Leptin enhances wound re-epithelialization and constitutes a direct function of leptin in skin repair. *J Clin Invest* 106:501-509.

Franke TF, Yang SI, Chan TO, Datta K, Kazlaukas A, Morrison DK, Kaplan DR and Tsichlis PN (1995) The protein kinase encoded by the Akt proto-oncogene is a target of the PDGF-activated phosphatidylinositol 3 kinase. *Cell* 81:727-736.

Friedman JM (2003) A war on obesity, not the obese. *Science* 299:856-858.

Green LC, Wagner DA, Glogowski J, Skipper PL, Wishnok JS, Tannenbaum SR (1982) Analysis of nitrate, nitrite and [^{15}N]nitrate in biological fluids. *Anal Biochem* 126:131-38.

Gordon S (2003) Alternative activation of macrophages. *Nat Rev Immunol* 3:23-35.

Goren I, Kämpfer H, Podda M, Pfeilschifter J and Frank S (2003) Leptin and wound inflammation in diabetic ob/ob mice: differential regulation of neutrophil and macrophage influx and a potential role for the scab as a sink for inflammatory cells and mediators. *Diabetes* 52:2821-2832.

Goren I, Müller E, Pfeilschifter J and Frank S (2006) Severely impaired insulin signaling in chronic wounds of diabetic ob/ob mice. A potential role of tumor necrosis factor-α. *Am J Pathol* 168:765-777.

Grau R, Punzon C, Fresno M and Iniguez MA (2006) Peroxisome-proliferator-activated receptor alpha agonists inhibit cyclo-oxygenase 2 and vascular endothelial growth factor transcriptional activation in human colorectal carcinoma cells via inhibition of activator protein-1. *Biochem J* 395:81-88.

He G, Sung YM and Fischer S (2006) Troglitazone induction of COX-2 expression is dependent on ERK activation in keratinocytes. *Prostaglandins Leukot Essent Fatty Acids* 74:193-197.

He G, Thuillier P and Fischer SM (2004) Troglitazone inhibits cyclin D1 expression and cell cycling independently of PPARgamma in normal mouse skin keratinocytes. *J Invest Dermatol* 123:1110-1119.

Henry RR (1997) Thiazolidinediones. *Endocrinol Metab Clin North Am* 26:553-573.

Hotamisligil GS (2006) Inflammation and metabolic disorders. *Nature* 444:860-867.

Kämpfer H, Pfeilschifter J and Frank S (2001) Expressional regulation of angiopoietin-1 and -2 and the tie-1 and -2 receptor tyrosine kinases during cutaneous wound healing: a comparative study of normal and impaired repair. *Lab Invest* 81:361-373.

Kanata S, Akagi M, Nishimura S, Hayakawa S, Yoshida K, Sawamura T, Munakata H and Hamanishi C (2006) Oxidized LDL binding to LOX-1 upregulates VEGF expression in cultured bovine chondrocytes through activation of PPAR-gamma. *Biochem Biophys Res Commun* 348:1003-10010.

Kliewer SA, Forman BM, Blumberg B, Ong ES, Borgmeyer U, Mangelsdorf DJ, Umesono K and Evans R (1994) Differential expression and activation of a family of murine peroxisome proliferator-activated receptors. *Proc Natl Acad Sci USA* 91:7355-7359.

Kliewer SA, Umesono K, Noonan DJ, Heyman RA and Evans R (1992) Convergence of 9-cis retinoic acid and peroxisome proliferator signalling pathways through heterodimer formation of their receptors. *Nature* 358:771-771.

Komuves LG, Hanley K, Lefebvre AM, Man MQ, Ng DC, Bikle DD Williams ML, Elias PM, Auwerx J and Feingold KR (2000) Stimulation of PPARalpha promotes epidermal keratinocyte differentiation in vivo. *J Invest Dermatol* 115:353-360.

Lehmann JM, Moore LB, Smith-Oliver TA, Wilkison WO, Willson TM and Kliewer SA (1995) An antidiabetic thiazolidinedione is a high affinity ligand for peroxisome proliferator-activated receptor gamma (PPAR gamma). *J Biol Chem* 270:12953-12956.

Mao-Qiang M, Fowler AJ, Schmuth M, Lau P, Chang S, Brown BE, Moser AH, Michalik L, Desvergne B, Wahli W, Li M, Metzger D, Chambon PH, Elias PM and Feingold KR (2004) Peroxisome proliferator-activated receptor (PPAR)-gamma activation stimulates keratinocyte differentiation. *J Invest Dermatol* 123:305-312.

Michalik L, Desvergne B, Tan NS, Basu-Modak S, Escher P, Rieusset J, Peters JM, Kaya G, Gonzalez FJ, Zakany J, Metzger D, Chambon P, Duboule D and Wahli W (2001) Impaired skin wound healing in peroxisome proliferator-activated receptor (PPAR)α and PPARβ mutant mice. *J Cell Biol* 154:799-814.

Michalik L and Wahli W (2007) Peroxisome proliferator-activated receptors (PPARs) in skin health, repair and disease. *Biochim Biophys Acta* 1771:991-998.

Mosmann T (1983) Rapid colorimetric assay for cellular growth and survival: Application to proliferation and cytotoxicity assays. *J Immunol Methods* 65:55-63

Panigrahy D, Singe S, Shen LQ, Butterfield CE, Freedman DA, Chen EJ, Moses MA, Kilroy S, Duensing S, Fletcher C, Fletcher JA, Hlatky L, Hahnfeldt P, Folkman and Kaipainen A (2002) PPARgamma ligands inhibit primary tumor growth and metastasis by inhibiting angiogenesis. *J Clin Invest* 110:923-932.

Peeters LL, Vigne JL, Tee MK, Zhao D, Waite L and Taylor RN (2005) PPARgamma represses VEGF expression in human endometrial cells: implications for uterine angiogenesis. *Angiogenesis* 8:373-379.

Piqueras L, Reynolds AR, Hodivala-Dilke KM, Alfranca A, Redondo JM, Hatae T, Tanabe T, Warner TD and Bishop-Bailey D (2007) Activation of PPARbeta/delta induces endothelial cell proliferation and angiogenesis. *Arterioscler Thromb Vasc Biol* 27:63-69.

Rangwala SM and Lazar MA (2004) Peroxisome proliferator-activated receptor γ in diabetes and metabolism. *Trends Pharmacol Sci* 25:331-336.

Rivier M, Safonova I, Lebrun P, Griffiths CE, Ailhaud G and Michel S (1998) Differential expression of peroxisome proliferator-activated receptor subtypes during the differentiation of human keratinocytes. *J Invest Dermatol* 111:1116-1121.

Singer AJ and Clark RAF (1999) Cutaneous wound healing. *New Engl J Med* 341:738-746.

Staels B and Fruchart JC (2005) Therapeutic roles of peroxisome proliferator-activated receptor agonists. *Diabetes* 54:2460-2470.

Stallmeyer B, Kämpfer H, Kolb N, Pfeilschifter J and Frank S (1999) The function of nitric oxide in wound repair: inhibition of inducible nitric oxide-synthase severely impairs wound reepithelialization. *J Invest Dermatol* 113:1090-1098.

Stallmeyer B, Pfeilschifter J and Frank S (2001) Systemically and topically supplemented leptin fails to reconstitute a normal angiogenic response during skin repair in diabetic ob/ob mice. *Diabetologia* 44:471-479.

Tilg H and Moschen AR (2006) Adipocytokines: mediators linking adipose tissue, inflammation and immunity. *Nat Rev Immunol* 6:772-783.

Wang D, Wang H, Guo Y, Ning W, Katkuri S, Wahli W, Desvergne B, Dey SK and DuBois RN (2006) Crosstalk between peroxisome proliferator-activated receptor delta and VEGF stimulates cancer progression. *Proc Natl Acad Sci USA* 103:19069-19074.

Molecular Pharmacology Fast Forward. Published on July 3, 2008 as DOI: 10.1124/mol.108.049395
This article has not been copyedited and formatted. The final version may differ from this version.

Footnotes

Dana Schiefelbein and Oliver Seitz contributed equally to this work. This work was supported by the Deutsche Forschungsgemeinschaft (SFB 553, grant FR 1540/1-2, GRK 1172). We are grateful to Dr. Elke Müller for determination of VEGF protein levels from mouse wound tissue.

Molecular Pharmacology Fast Forward. Published on July 3, 2008 as DOI: 10.1124/mol.108.049395
This article has not been copyedited and formatted. The final version may differ from this version.

Figure legends

Figure 1. Dose-dependent induction of VEGF expression in keratinocytes by PPAR agonists. Quiescent human HaCaT keratinocytes were stimulated with troglitazone (*a*), rosiglitazone (*b*), or L165,041 (*c*) for 24 h as indicated. EGF (10 ng/ml) was used as a control. After 24 h, VEGF mRNA expression of non-stimulated (*ctrl*) or stimulated keratinocytes was analyzed by RNase protection assay (*upper and middle panels*). $VEGF_{165}$ protein release from the cells was assessed by ELISA analyses of the corresponding conditioned cell culture supernatants (*lower panels*). **, $P < 0.01$; *, $P < 0.05$; n.s., not significant as compared to non-stimulated control cells (*ctrl*). Bars indicate the mean ± SD from three independent cell culture experiments (n=3).

Figure 2. Time-dependent induction of VEGF expression in keratinocytes by PPAR agonists. Confluent human HaCaT keratinocytes were stimulated with 25 µM troglitazone (*a*), or 50 µM L165,041 (*b*) for the indicated time points. At the indicated time points of stimulation, VEGF mRNA expression of non-stimulated (*ctrl 0h*) or stimulated keratinocytes was analyzed by RNase protection assay (*upper and middle panels*). $VEGF_{165}$ protein release from the cells was assessed by ELISA analyses of the corresponding conditioned cell culture supernatants (*lower panels*). **, $P < 0.01$; *, $P < 0.05$ as compared to non-stimulated control cells (*ctrl*). Bars indicate the mean ± SD from three independent cell culture experiments (n=3).

Figure 3. Rosiglitazone and troglitazone are functionally active. Quiescent murine RAW264.7 macrophages were activated using LPS (200 ng/ml) and IFNγ (2 ng/ml) for 24 h in the presence or absence of 50 µM rosiglitazone (*a*) or 25 µM troglitazone (*b*). Nitrite accumulation as a readout of iNOS activity and thus macrophage activation was assessed using the Griess reaction. **, $P < 0.01$; *, $P < 0.05$ as indicated by the bracket. Bars indicate the mean ± SD from three independent cell culture experiments (n=3).

Molecular Pharmacology Fast Forward. Published on July 3, 2008 as DOI: 10.1124/mol.108.049395
This article has not been copyedited and formatted. The final version may differ from this version.

Figure 4. Induction of VEGF expression by PPARβ/δ and PPARγ agonists in human primary keratinocytes. Quiescent human primary keratinocytes were stimulated with EGF (10 ng/ml), troglitazone (25 μM), or L165,041 (50 μM) for 24 h. After 24 h, VEGF mRNA expression of non-stimulated (*ctrl*) or stimulated primary keratinocytes was analyzed by RNase protection assay (*a*). **, $P < 0.01$ as compared to non-stimulated control cells (*ctrl*). Bars indicate the mean ± SD from three independent cell culture experiments (n=3). $VEGF_{165}$ protein release from the cells was assessed by ELISA analyses of conditioned cell culture supernatants (*b*). $VEGF_{165}$ protein expression from one representative experiment is shown.

Figure 5. PPARβ/δ and PPARγ agonists do not stabilize VEGF mRNA. Quiescent HaCaT keratinocytes were stimulated with EGF (10 ng/ml), troglitazone (25 μM), or L165,041 (50 μM) for 16 h. After 16 h, actinomycin D (*ActD*, 10 μM) was added to the cells. Keratinocyte VEGF mRNA levels were determined at the indicated time points of treatment by RNase protection assay. Bars indicate the mean ± SD from three independent cell culture experiments (n=3). A RNase protection assay demonstrating VEGF mRNA in stimulated keratinocytes in the absence of *ActD* (16h and 24 h as indicated) is shown in the *lower panel*.

Figure 6. Troglitazone- and L165,041-mediated VEGF expression is dependent on MAPK activation. Quiescent human HaCaT keratinocytes were stimulated with troglitazone (*a*), or L165,041 (*b*) for 16 h and 24 h in the absence or presence of wortmannin (*WTM*, 200 nM), SB203580 (5 μM), or U0126 (10 μM) as indicated and subsequently analyzed for VEGF mRNA expression by RNase protection assay (*upper and middle panels*). $VEGF_{165}$ protein release from the cells was assessed by ELISA analyses of the corresponding conditioned cell culture supernatants (*lower panels*). **, $P < 0.01$; *, $P < 0.05$ as compared to stimulated keratinocytes in the absence of the respective inhibitor. Bars indicate the mean ± SD from three independent cell culture experiments (n=3).

Molecular Pharmacology Fast Forward. Published on July 3, 2008 as DOI: 10.1124/mol.108.049395
This article has not been copyedited and formatted. The final version may differ from this version.

Figure 7. Differential activation of p38 and p42/44 MAPK by PPAR agonists. (*a*), quiescent HaCaT keratinocytes were treated with L165,041 (50 µM), troglitazone (25 µM), or rosiglitazone (50 µM) for the indicated time periods. Non-stimulated cells (*ctrl 0', ctrl 90'*) served as controls. Total cell lysates were analyzed for the presence phosphorylated p38 MAPK (*p-p38 Thr180, Tyr182*) or phosphorylated p42/44 MAPK (*p-p42/44 Thr202, Tyr204*) by immunoblot. Loading of gels was controlled by analysis of β-actin expression as indicated. (*b*), keratinocyte viability as assessed by MTT assay in the presence or absence of troglitazone (25 µM), rosiglitazone (50µM), or L165,041 (50 µM) as indicated. **, $P < 0.01$; *, $P < 0.05$; n.s., not significant as compared to non-stimulated control cells (*ctrl*). Bars indicate the mean ± SD from three independent cell culture experiments (n=3).

Figure 8. Troglitazone- and L165,041-induced VEGF expression are independent of PPAR expression. Cultured HaCaT keratinocytes were treated with oligofectamine® alone (*ctrl*) and in combination with a non-specific (*scrambled*) siRNA, a PPARγ-specific siRNA (*si-PPARγ*) (*a*) or a PPARβ/δ-specific siRNA (si-PPARβ/δ) (*b*) as indicated. Abrogation of the respective PPAR in keratinocytes was controlled by immunoblot (*a, left panel*) or RNase protection assay (*b, left panel*) as indicated. Analysis of β-actin (*a*) or GAPDH (*b*) was used to control an equal loading. $VEGF_{165}$ protein release from control- (*ctrl*), scrambled RNA (*scr*)- or PPAR-specific siRNA (*si-Pγ; si-Pβ/δ*)-treated keratinocytes in the absence (*w/o*) or presence (+) of troglitazone (25 µM) or L165,041 (50 µM) as indicated. **, $P < 0.01$ as compared to conditions without drug. ##, $P < 0.01$; n.s., not significant as indicated by brackets. Bars indicate the mean ± SD from three independent cell culture experiments (n=3).

Figure 9. Impaired VEGF protein expression in acute wounds of diabetic mice. VEGF ELISA analyses from lysates of nonwounded skin (*ctrl*) and lysates of wound tissue isolated from wildtype (*C57Bl/6J*) and diabetic *ob/ob* mice. VEGF protein is expressed as pg/50 µg

Molecular Pharmacology Fast Forward. Published on July 3, 2008 as DOI: 10.1124/mol.108.049395
This article has not been copyedited and formatted. The final version may differ from this version.

skin or wound lysate. **, $P < 0.01$; *, $P < 0.05$; n.s., not significant (unpaired Student's *t* test). Bars indicate the mean ± SD obtained from wound lysates from 12 individual mice (n=12).

Figure 10. Rosiglitazone impairs VEGF expression from keratinocytes in acute wounds of *ob/ob* mice. (*a*), VEGF mRNA expression in total wound tissue of non-treated (*mock*) or rosiglitazone (*rosi*)-administered *ob/ob* mice was determined 1 day (*1 d wound tissue*) or 5 days (*5 d wound tissue*) upon injury by RNase protection assay. Expression levels of VEGF mRNA are expressed as arbitrary PhosphoImager PSL units. *, $P < 0.05$ as compared to non-wounded control skin (ctrl) (ANOVA, Dunett's method). Bars indicate the mean ± SD from four wounds (n=4) from three individual mice (n=3). (*b*), overview to show tissue sampling for inner wound (*iw*) and wound margin (*m*) compartments (*left panel*). RNase protection analysis of VEGF mRNA levels in wound margin (*wm*) and inner wound (*iw*) tissue compartments isolated from mock (*mock*)- or rosiglitazone (*rosi*)-treated *ob/ob* mice 1 day (*1 d wd*) and 5 days (*5 d wd*) upon injury. *Ctrl skin* refers to back skin biopsies of non-wounded mice. A *tRNA* was used to control specificity of the VEGF antisense RNA. A simultaneous hybridization of GAPDH within the same samples served to control an equal loading. Every experimental time point depicts isolated *wm* and *iw* compartments from two wounds each (n=2) obtained from three individual mice (n=3), which have been pooled prior to analysis. (*c*), paraffin-fixed sections from mouse wounds (day 5 post-wounding) were incubated with a polyclonal goat antiserum directed against murine VEGF. Immunopositive signals within the sections are indicated with *arrows*. Wound margin epithelia are indicated by a red line. *ac*, adipocytes; *gt*, granulation tissue; *he*, hyperproliferative epithelium; *sc*, scab.

Figure 11. Differential effects of PPARγ agonists in diabetes-impaired wound tissue: MAPK activation. Total wound tissue of non-treated (*mock*), or rosiglitazone- (*rosi*)- and troglitazone (*trogli*)- administered *ob/ob* mice was analyzed for the presence of phosphorylated p38 MAPK (*p-p38, Thr180, Tyr182*) or phosphorylated p42/44 MAPK (*p-*

Molecular Pharmacology Fast Forward. Published on July 3, 2008 as DOI: 10.1124/mol.108.049395
This article has not been copyedited and formatted. The final version may differ from this version.

p42/44, Thr202, Tyr204) by immunoblot. *Mouse #1, #2* or *#3* represent individual mice. Every experimental time point depicts two wounds (n=2) obtained from an individual mouse, which have been pooled prior to analysis. β-actin was used to control loading.

Figure 12. Differential effects of PPARγ agonists in diabetes-impaired wound tissue: histology. Paraffin-fixed sections from mouse wounds (day 5 post-wounding) were incubated with antisera directed against murine VEGF (*upper panel*) or murine phosphorylated p38 MAPK (*panels 2-4*). Immunopositive signals within the sections are indicated with *arrows*. Wound margin epithelia are indicated by a red line. *ac*, adipocytes; *gt*, granulation tissue; *he*, hyperproliferative epithelium; *sc*, scab. Scale bar = 100 µM.

Figure 13. PPARγ agonists do not interfere with cytokine- and EGF-induced VEGF expression in keratinocytes. (a), quiescent human HaCaT keratinocytes were stimulated with increasing concentrations of cytokines (1= TNFα: 25 ng/ml, IL-1β: 50 ng/ml; IFNγ: 10 ng/ml) (*a*) or EGF (0,1-10 ng/ml) (*b*) as indicated to determine the EC_{50}. After 24 h, $VEGF_{165}$ protein release from the cells was assessed by ELISA analyses of the corresponding conditioned cell culture supernatants (*upper panels*). Cells were subsequently stimulated with EC_{50} doses of cytokines (*a, lower panels*) or EGF (*b, lower panels*) in the presence or absence of troglitazone or rosiglitazone as indicated. **, $P < 0.01$ as compared to non-stimulated control cells (*ctrl*). Bars indicate the mean ± SD from three independent cell culture experiments (n=3).

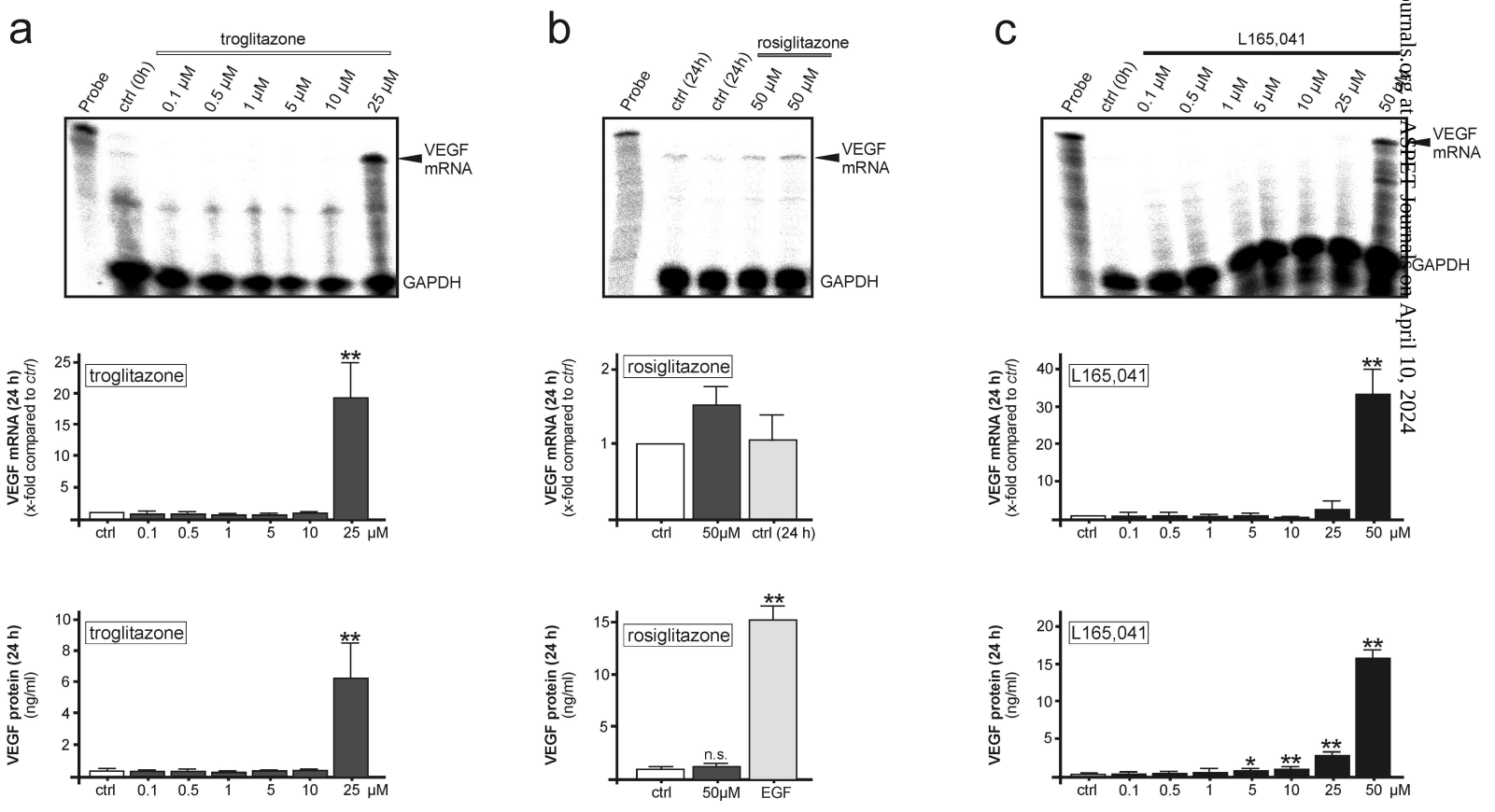

Figure 1

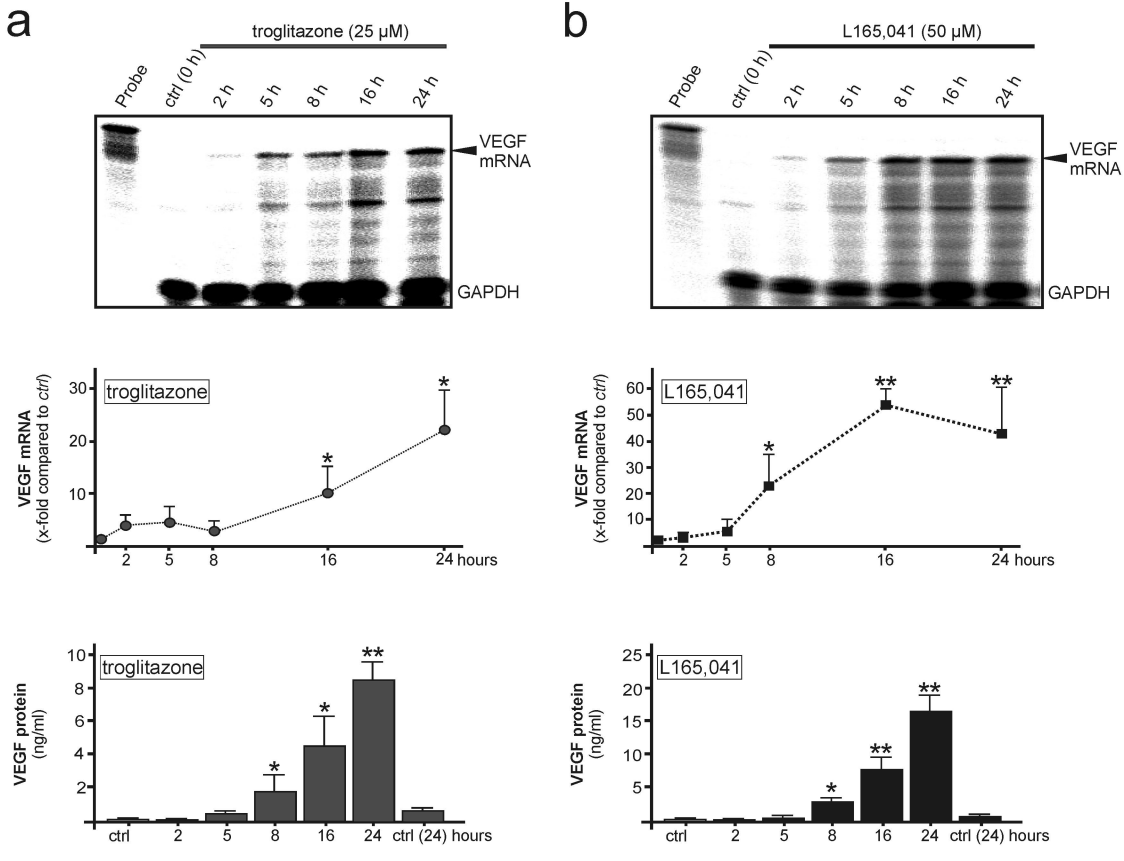
a
troglitazone (25 μM)
Probe
ctrl (0 h)
2 h
5 h
8 h
16 h
24 h
VEGF mRNA
GAPDH
b
L165,041 (50 μM)
Probe
ctrl (0 h)
2 h
5 h
8 h
16 h
24 h
VEGF mRNA
GAPDH
troglitazone
VEGF mRNA (x-fold compared to ctrl)
2
5
8
16
24 hours
L165,041
VEGF mRNA (x-fold compared to ctrl)
2
5
8
16
24 hours
troglitazone
VEGF protein (ng/ml)
ctrl
2
5
8
16
24
ctrl (24) hours
L165,041
VEGF protein (ng/ml)
ctrl
2
5
8
16
24
ctrl (24) hours

Figure 2

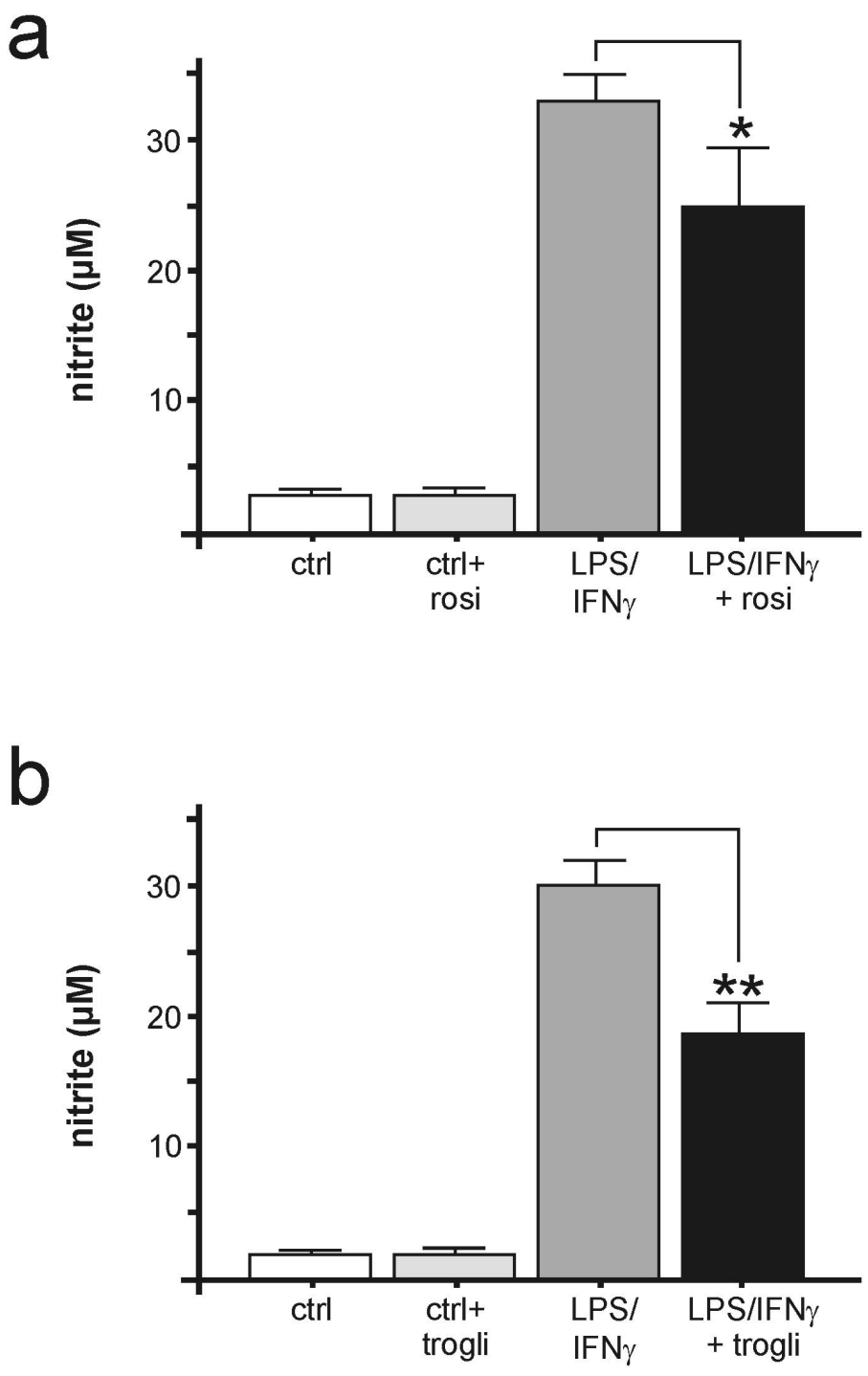
a
nitrite (µM)
30
20
10
*
ctrl
ctrl+ rosi
LPS/ IFNγ
LPS/IFNγ + rosi
b
nitrite (µM)
30
20
10
**
ctrl
ctrl+ trogli
LPS/ IFNγ
LPS/IFNγ + trogli

Figure 3

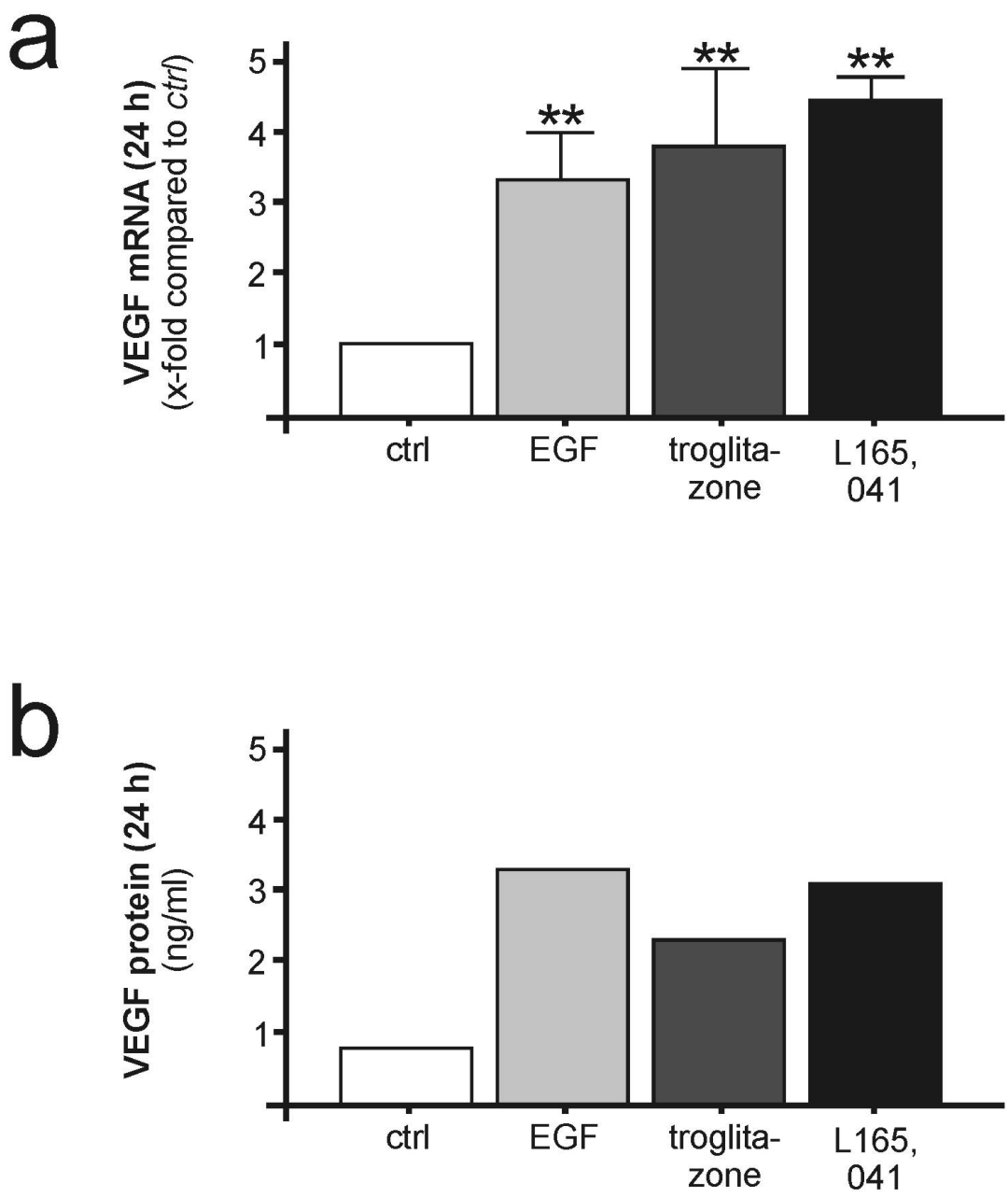
a
VEGF mRNA (24 h)
(x-fold compared to ctrl)
5
4
3
2
1
**
**
**
ctrl
EGF
troglita-
zone
L165,
041
b
VEGF protein (24 h)
(ng/ml)
5
4
3
2
1
ctrl
EGF
troglita-
zone
L165,
041

Figure 4

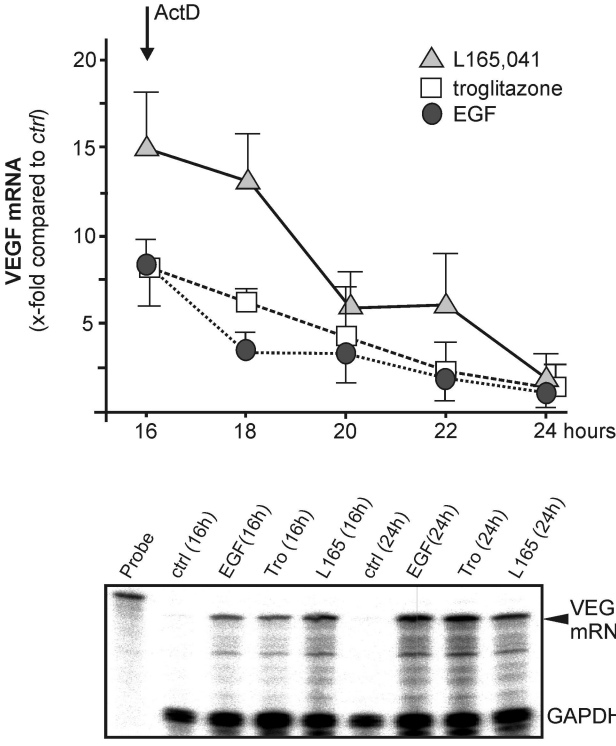
ActD
L165,041
troglitazone
EGF
VEGF mRNA
(x-fold compared to ctrl)
20
15
10
5
16
18
20
22
24 hours
Probe
ctrl (16h)
EGF(16h)
Tro (16h)
L165 (16h)
ctrl (24h)
EGF(24h)
Tro (24h)
L165 (24h)
VEGF mRNA
GAPDH

Figure 5

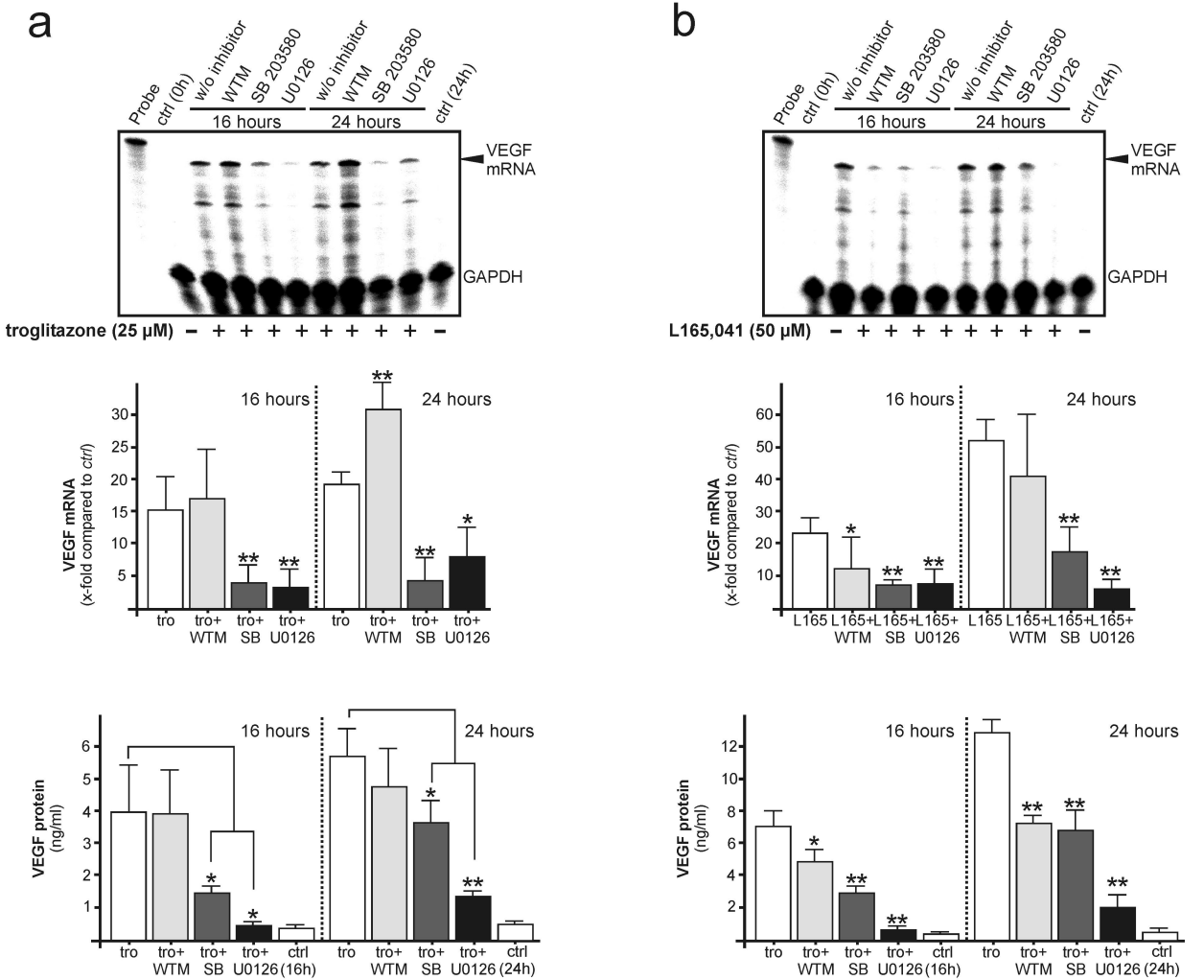
a
b
Probe
ctrl (0h)
w/o inhibitor
WTM
SB 203580
U0126
16 hours
24 hours
ctrl (24h)
VEGF mRNA
GAPDH
troglitazone (25 μM)
L165,041 (50 μM)
VEGF mRNA (x-fold compared to ctrl)
VEGF protein (ng/ml)
tro
tro+ WTM
tro+ SB
tro+ U0126
ctrl (16h)
ctrl (24h)
L165
L165+ WTM
L165+ SB
L165+ U0126

Figure 6

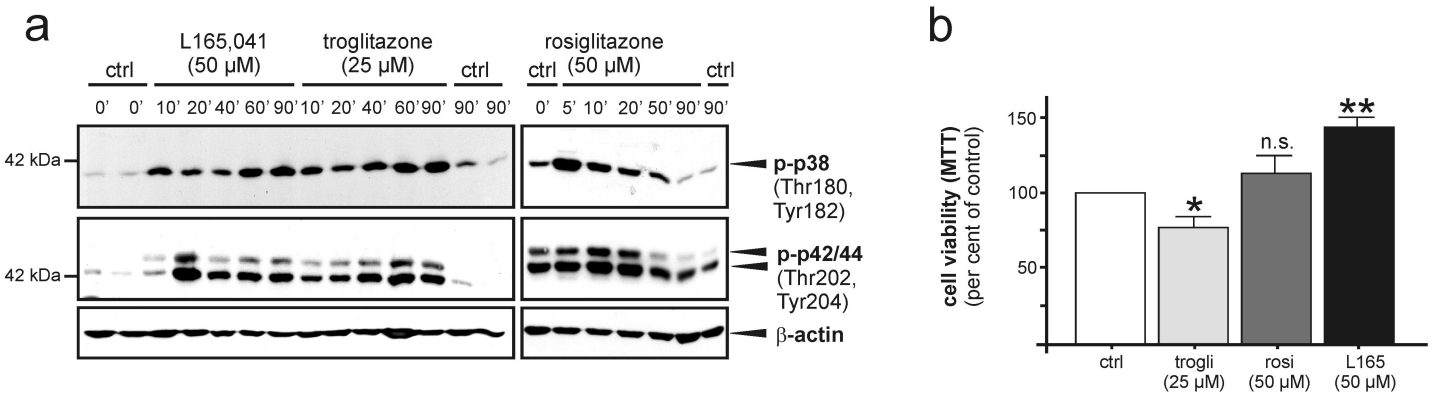

Figure 7

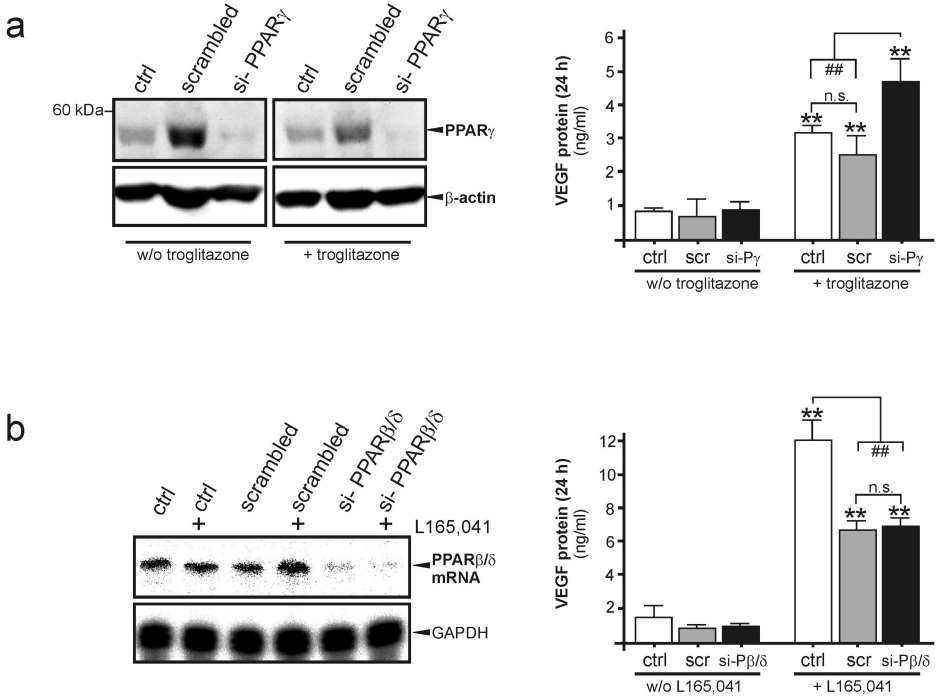
a
ctrl
scrambled
si- PPARγ
ctrl
scrambled
si- PPARγ
60 kDa
PPARγ
β-actin
w/o troglitazone
+ troglitazone
VEGF protein (24 h)
(ng/ml)
6
5
4
3
2
1
##
n.s.
**
**
**
**
ctrl
scr
si-Pγ
ctrl
scr
si-Pγ
w/o troglitazone
+ troglitazone
b
ctrl
ctrl
+
scrambled
scrambled
+
si- PPARβ/δ
si- PPARβ/δ
+
L165,041
PPARβ/δ
mRNA
GAPDH
VEGF protein (24 h)
(ng/ml)
12
10
8
6
4
2
**
##
n.s.
**
**
ctrl
scr
si-Pβ/δ
ctrl
scr
si-Pβ/δ
w/o L165,041
+ L165,041

Figure 8

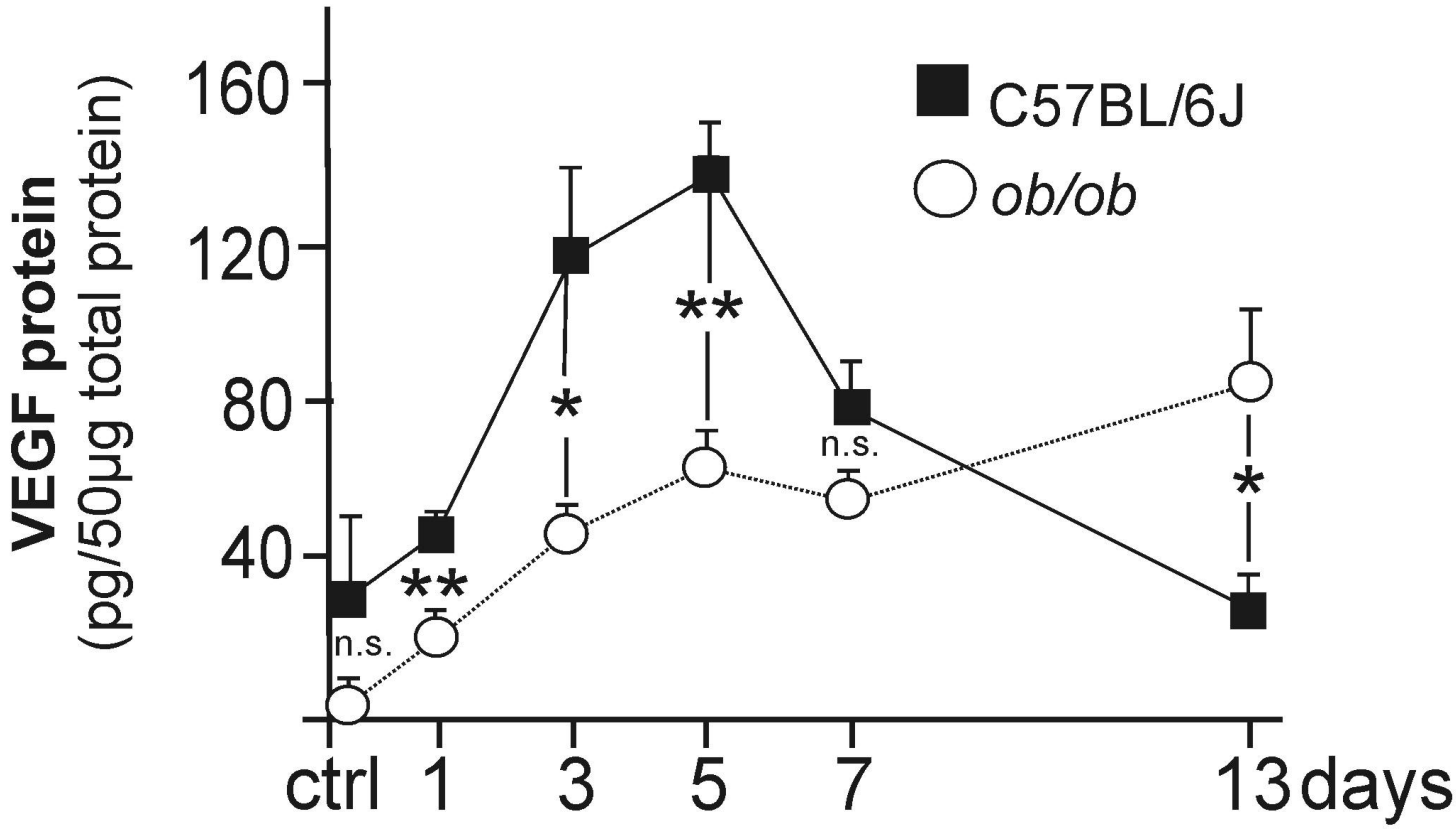
VEGF protein
(pg/50µg total protein)
160
120
80
40
C57BL/6J
ob/ob
n.s.
**
*
**
n.s.
*
ctrl
1
3
5
7
13
days

Figure 9

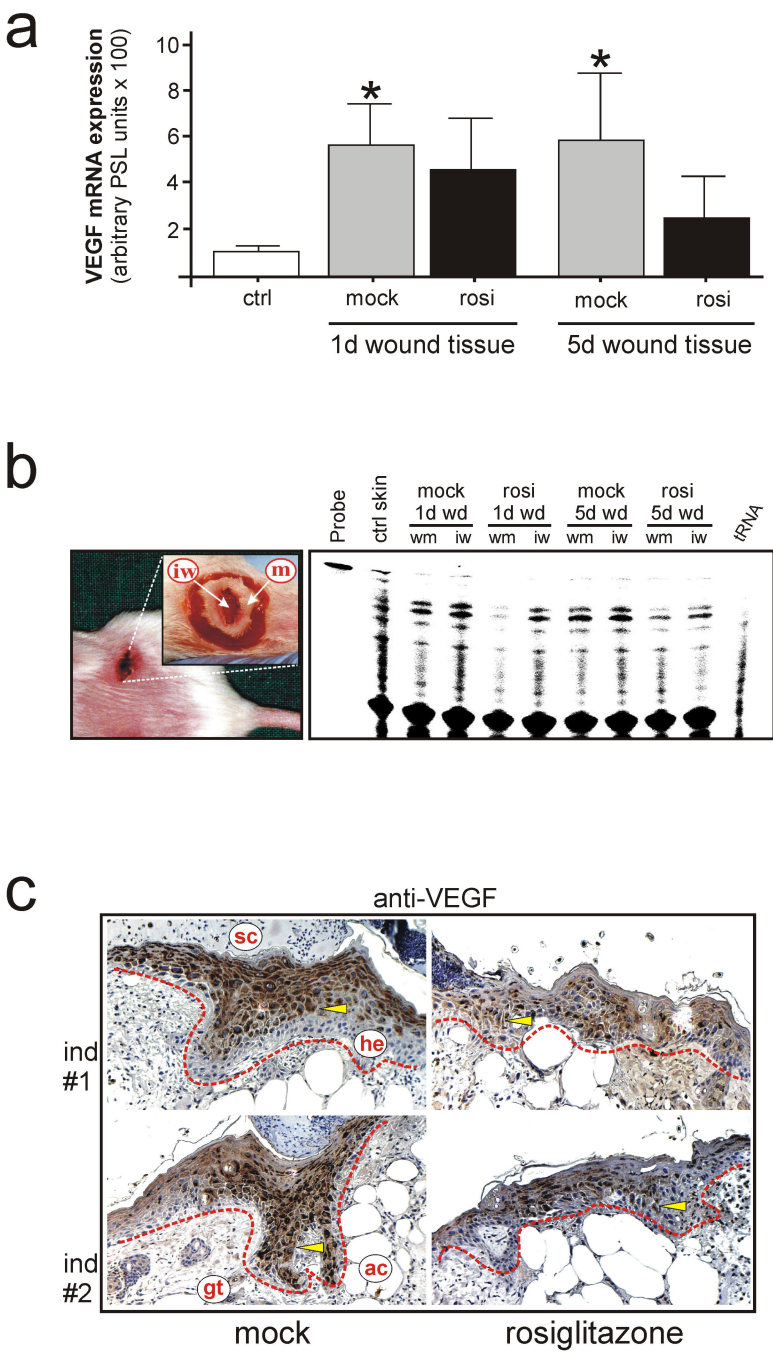
a
VEGF mRNA expression
(arbitrary PSL units x 100)
10
8
6
4
2
*
*
ctrl
mock
rosi
mock
rosi
1d wound tissue
5d wound tissue
b
Probe
ctrl skin
mock 1d wd
rosi 1d wd
mock 5d wd
rosi 5d wd
wm iw wm iw wm iw wm iw
tRNA
iw
m
VEGF mRNA
GAPDH
c
anti-VEGF
sc
he
ind #1
ind #2
gt
ac
mock
rosiglitazone

Figure 10

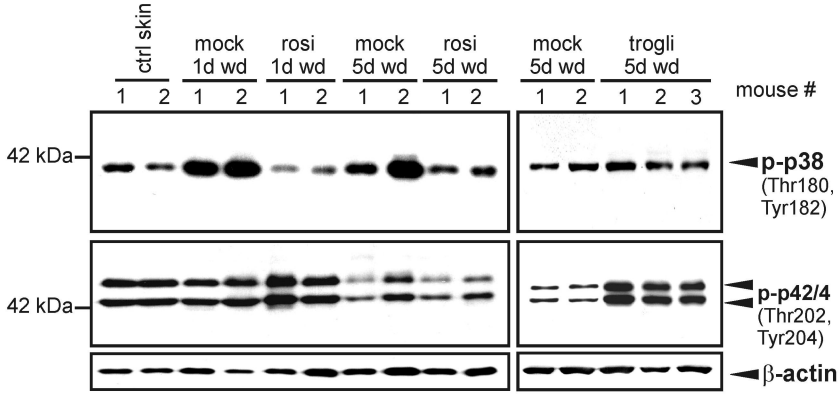
ctrl skin
mock 1d wd
rosi 1d wd
mock 5d wd
rosi 5d wd
mock 5d wd
trogli 5d wd
mouse #
1 2 1 2 1 2 1 2 1 2 1 2 1 2 3
42 kDa
p-p38 (Thr180, Tyr182)
42 kDa
p-p42/4 (Thr202, Tyr204)
β-actin

Figure 11

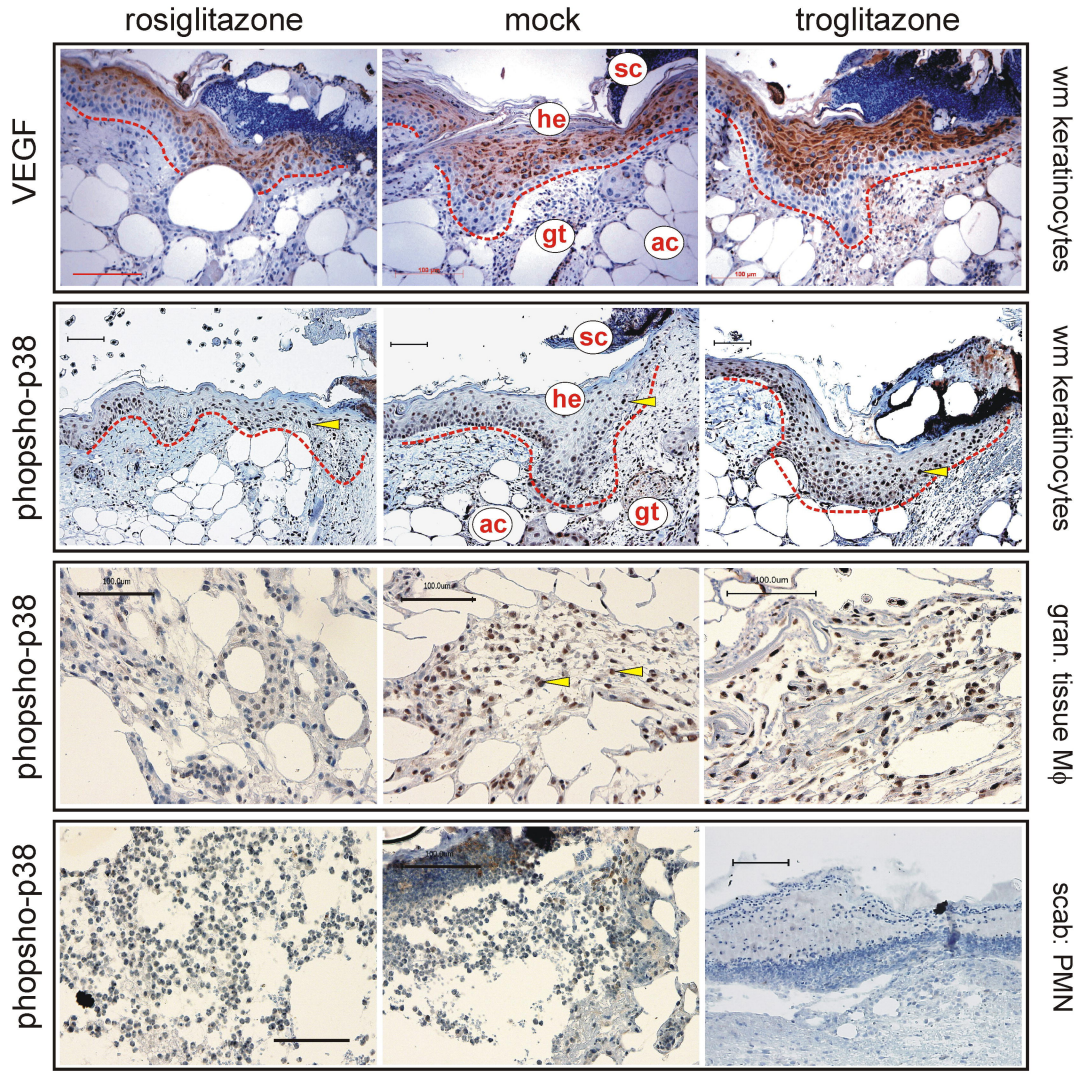
rosiglitazone
mock
troglitazone
VEGF
phopsho-p38
phopsho-p38
phopsho-p38
wm keratinocytes
wm keratinocytes
gran. tissue Mϕ
scab: PMN
sc
he
gt
ac
sc
he
ac
gt

Figure 12

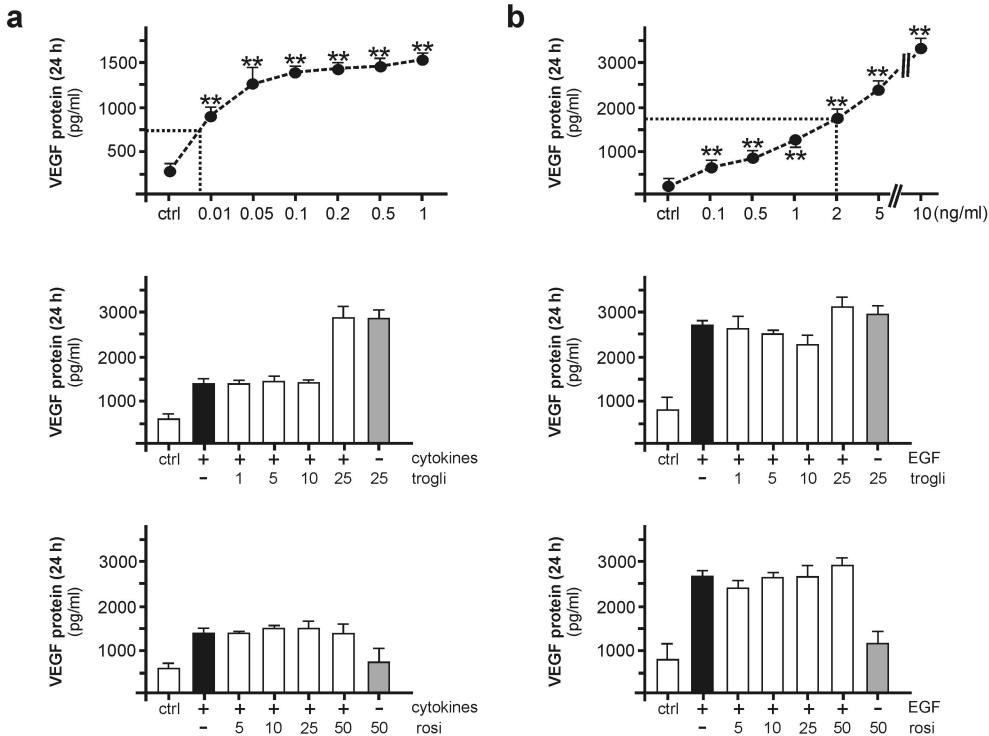
a
b
VEGF protein (24 h) (pg/ml)
1500
1000
500
ctrl 0.01 0.05 0.1 0.2 0.5 1
3000
2000
1000
ctrl 0.1 0.5 1 2 5 10 (ng/ml)
ctrl + + + + + - cytokines
- 1 5 10 25 25 trogli
ctrl + + + + + - EGF
- 1 5 10 25 25 trogli
ctrl + + + + + - cytokines
- 5 10 25 50 50 rosi
ctrl + + + + + - EGF
- 5 10 25 50 50 rosi

Figure 13